Electronic Supplementary Information

In situ growth of TiO_2 layer on flexible Ti substrate targeting interface recombination issue of $BiVO_4$ photoanodes for efficient solar water splitting

Jiuwang Gu, [a] Qitong Huang, [a] Kai-Hang Ye, [c] Yufei Yuan, [a] Zilong Wang [*a] and Wenjie Mai [*ab]

[a.] *Siyuan Laboratory, Guangzhou Key Laboratory of Vacuum Coating Technologies and New Energy Materials, Department of Physics, Jinan University, Guangzhou, Guangdong 510632, China.*Email:* wenjiemai@gmail.com
[b.] *Guangdong Provincial Key Laboratory of Optical Fiber Sensing and Communications, Jinan University, Guangzhou 510632, People's Republic of China.*
[c.] *Department of Chemistry, Jinan University, Guangzhou, Guangdong 510632, China.*

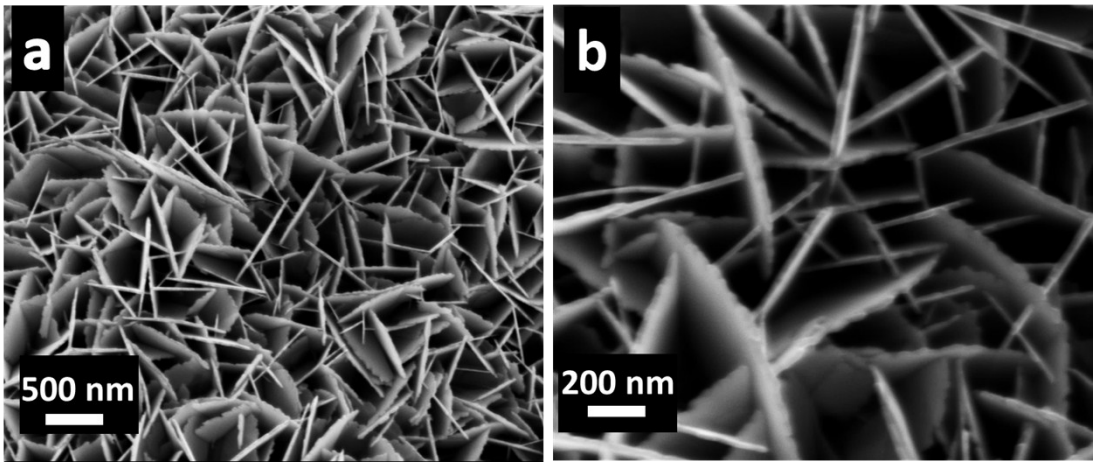

Fig. S1 SEM images of Ti foil-BiOI electrode at low (a) and high (b) magnifications.

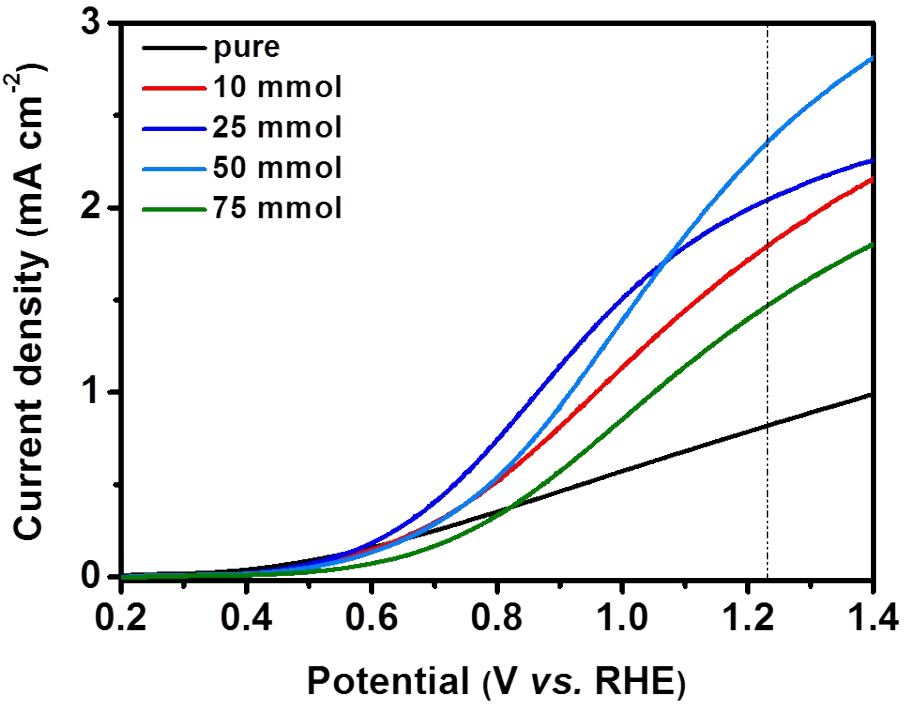

Fig. S2 *J-V* curves of Mo-$BiVO_4$ photoanodes based on Ti substrate varied from concentration of molybdenum source measured in 0.1 M phosphate buffer solution (pH 7.4).

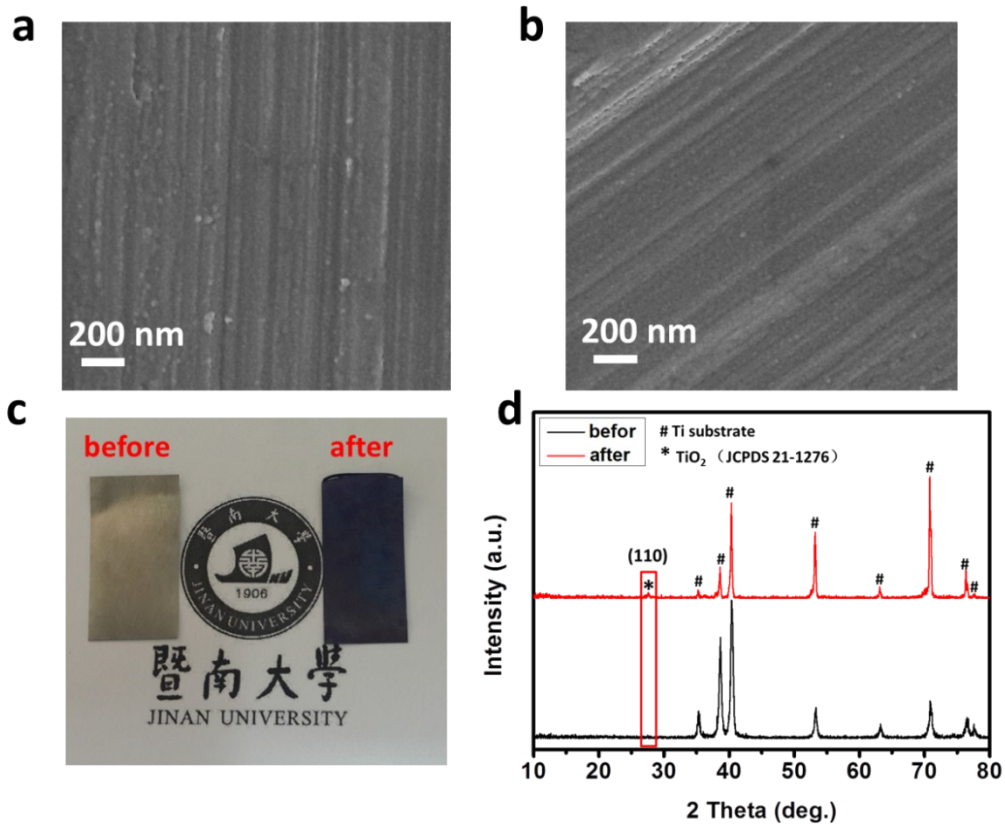

Fig. S3 SEM images of Ti foil before (a) and after (b) annealing process. Digital photographs (c) and XRD patterns (d) of non-annealed Ti foil and annealed Ti foil samples. When comparing the SEM images of Ti foil before and after the annealing treatment, one can notice that the surface turns to be compact and smooth for the annealed Ti foil. The XRD pattern of annealed Ti foil also shows one weak peak of TiO_2 (JCPDS 21-1276), confirming the in-situ growth of TiO_2 on the Ti substrate after the annealing process.

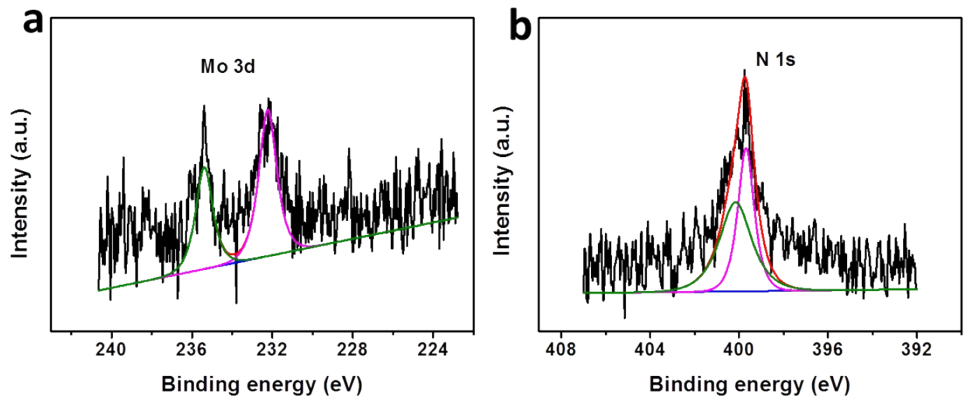

Fig. S4 XPS spectra of (a) Mo_{3d} and (b) N_{1s} peaks from the Mo, N-$BiVO_4$ sample.

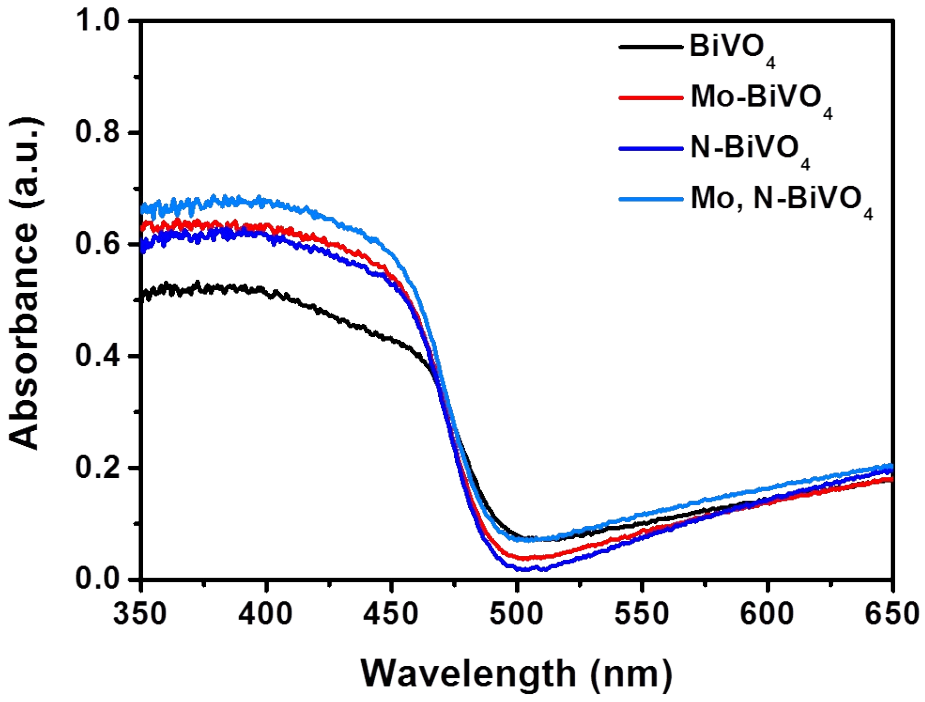

Fig. S5 UV-vis absorption spectra of pristine and modified $BiVO_4$ photoanodes based on Ti substrate.

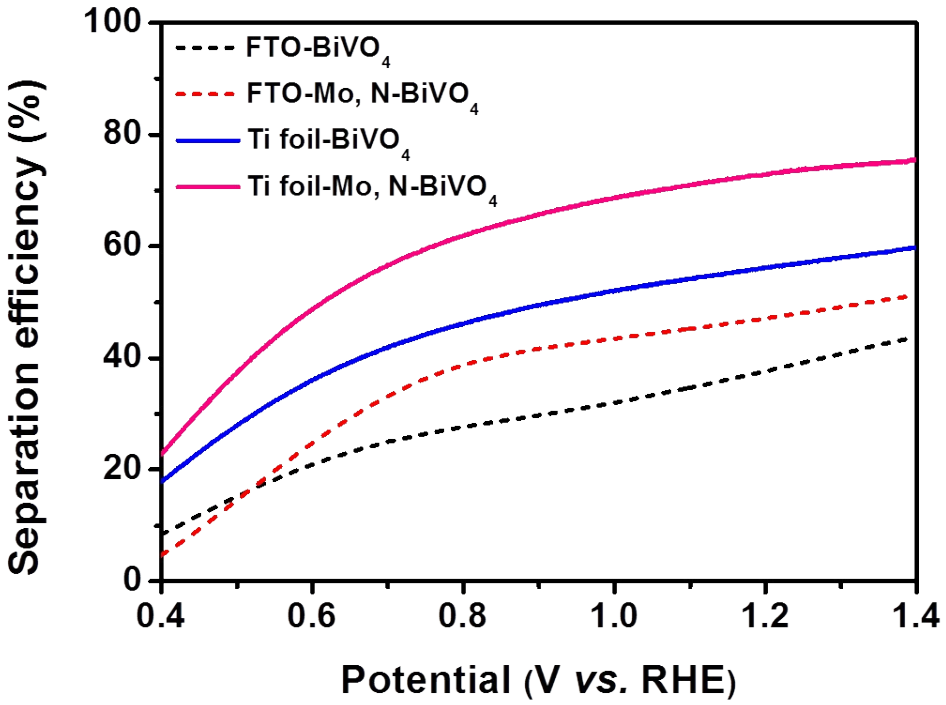

Fig. S6 Charge separation efficiency (η_{sep}) of $BiVO_4$ and co-doped $BiVO_4$ photoanodes based on FTO substrate and Ti substrate, respectively.

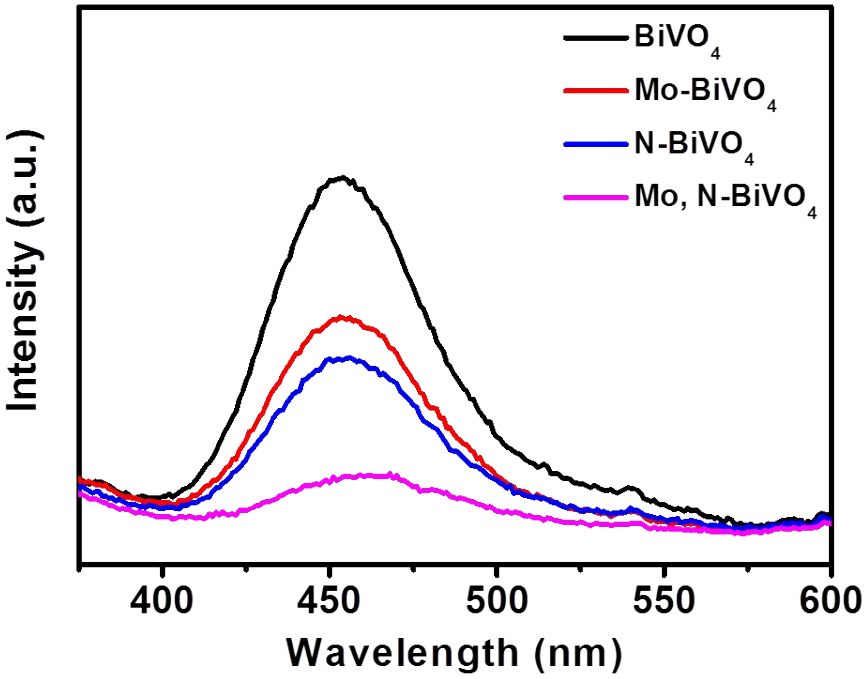

Fig. S7 PL spectra of pristine and modified $BiVO_4$ photoanodes based on Ti substrate (with excitation wavelength of 330 nm).

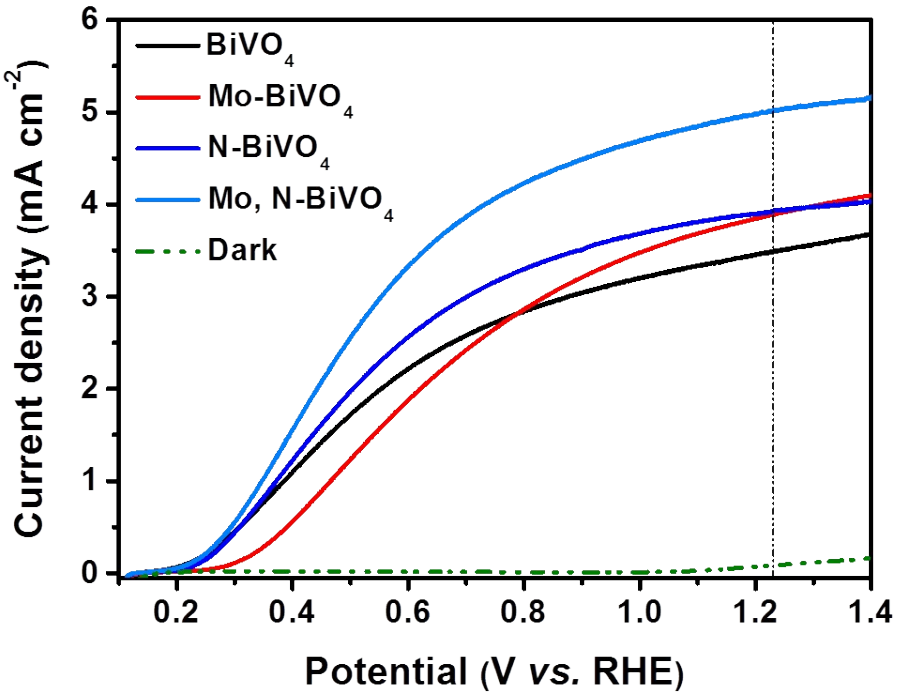

Fig. S8 *J-V* curves of pristine and modified $BiVO_4$ photoanodes based on Ti substrate for solar sulfite oxidation collected under AM 1.5G illumination in 0.1 M phosphate buffer solution (pH 7.4) containing 1 M Na_2SO_3 as hole scavenger.

Table S1. Fitting equivalent circuit and EIS fitting results of pristine and modified $BiVO_4$ photoanodes based on Ti substrate.

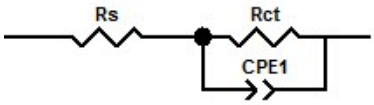

Sample	$BiVO_4$	Mo-$BiVO_4$	N-$BiVO_4$	Mo, N-$BiVO_4$
R_s (Ω)	44	33	48	35
CPE-T (μF)	180	205	206	273
CPE-T (μF)	0.75	0.83	0.80	0.82
R_{ct} (kΩ)	40.90	15.22	18.78	0.38

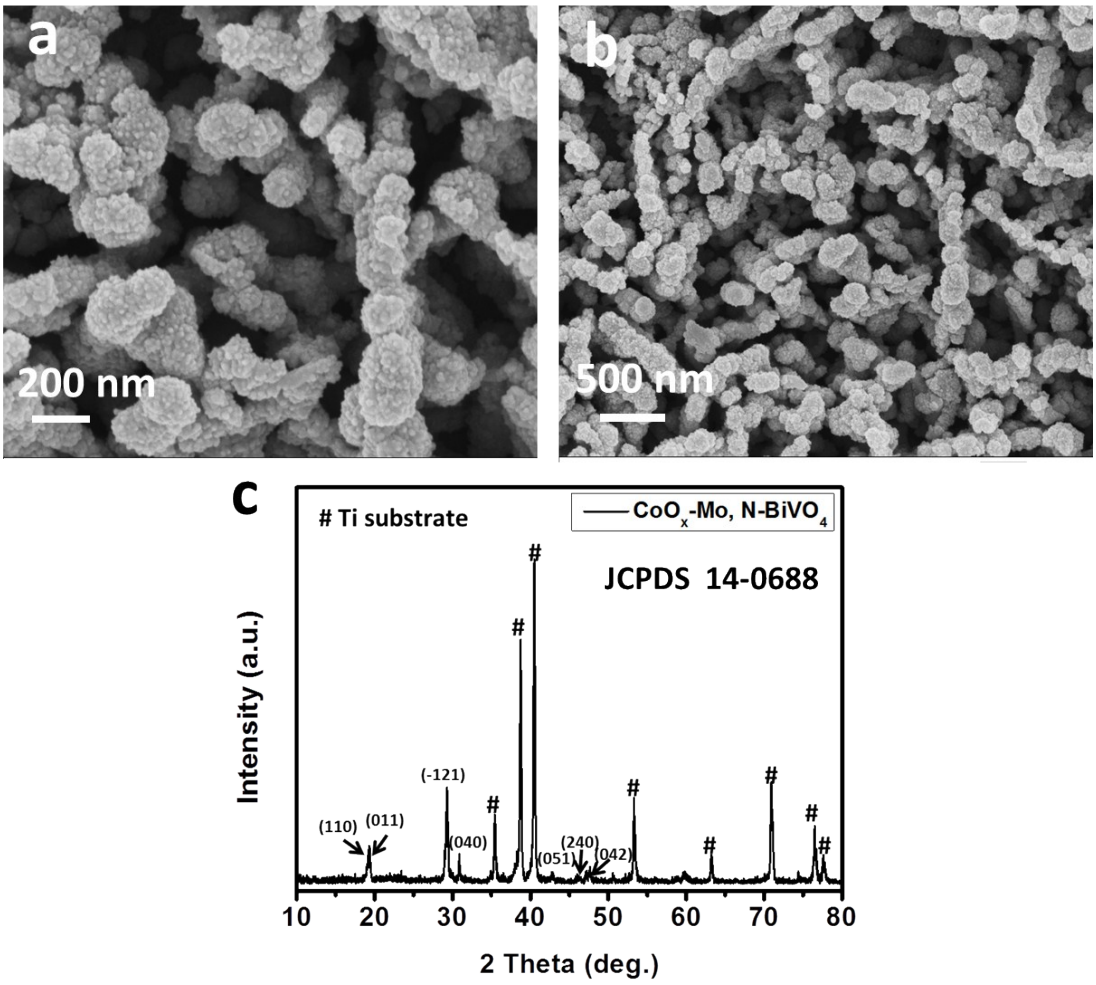

Fig. S9 SEM images at high (a) and low magnifications (b) and XRD pattern (c) of the CoO_x-Mo, N-$BiVO_4$ sample.

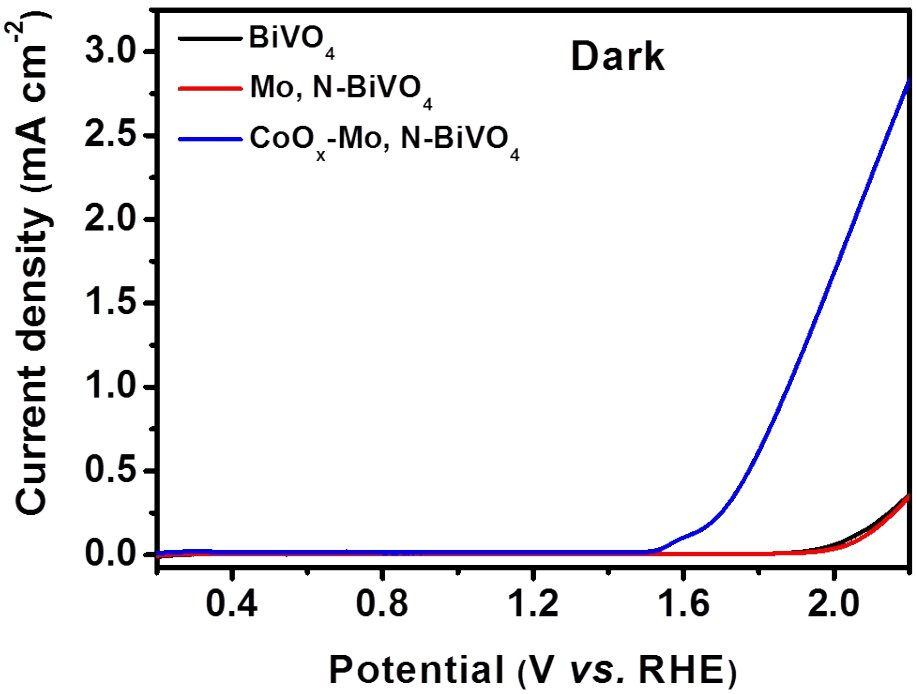

Fig. S10 *J-V* curves of pristine and modified $BiVO_4$ photoanodes based on the Ti substrate for electrical water oxidation collected in dark. The cathodic shift of the dark current onset potential for CoO_x-Mo, N-$BiVO_4$ indicates the excellent OER kinetics of CoO_x catalyst for electrochemical water splitting. A 0.1 M phosphate buffer solution (pH 7.4) was used as the electrolyte.

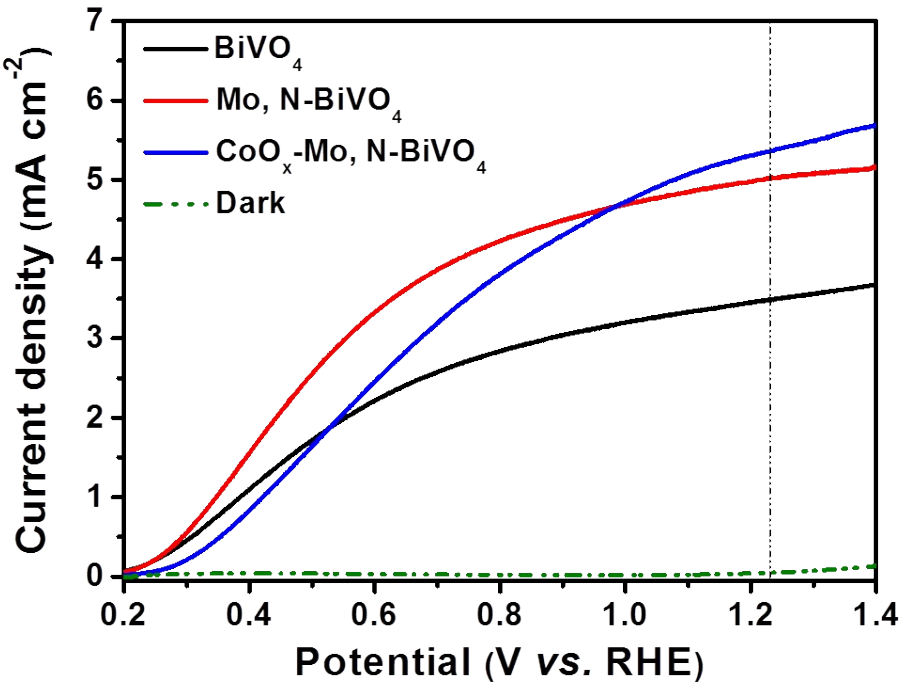

Fig. S11 *J-V* curves of the pristine $BiVO_4$, Mo, N-$BiVO_4$ and CoO_x-Mo, N-$BiVO_4$ photoanodes based on Ti substrate for solar sulfite oxidation collected under AM 1.5G illumination in 0.1 M phosphate buffer solution (pH 7.4) containing 1 M Na_2SO_3 as hole scavenger.

Table S2. Summary of recent key advances in $BiVO_4$ based photoanodes for PEC solar water splitting.

Photoanodes	Substrate	Photocurrent density at 1.23 V_{RHE}	ABPE value	Ref.
$BiOI/BiVO_4$	FTO glass	3.27 mA cm^{-2}	0.97%	(5)
$FeOOH\text{-}NiOOH/N\text{-}BiVO_4$	FTO glass	~5 mA cm^{-2}	2.2%	(7)
Co-Pi/W: $BiVO_4$	FTO glass	~1.4 mA cm^{-2}	~	(9)
$NiFeO_x$-Bi-$BiVO_4$ (two electrode stack)	ITO glass	~5 mA cm^{-2}	2.25%	(10)
$BiVO_4/FeOOH/NiOOH$	FTO glass	2.73 mA cm^{-2} at 0.6 V_{RHE}	1.75%	(11)
$CoPi/BiVO_4/TiO_2$	FTO glass	1.61 mA cm^{-2}	~	(14)
Mo-$BiVO_4$	FTO glass	1.2 mA cm^{-2}	~	(15)
$NiO/CoO_x/BiVO_4$	ITO glass	2.5 mA cm^{-2} at 0.6 V_{RHE}	1.5%	(16)
$BiVO_4/WO_3/SnO_2$	FTO glass	2 mA cm^{-2}	~	(17)
$NiO/CoO_x/BiVO_4$	Ti	3.5 mA cm^{-2}	1.5%	(23)
$NiOOH/FeOOH/CQDs/BiVO_4$	FTO glass	5.99 mA cm^{-2}	2.29%	(29)
CoO_x-Mo, N-$BiVO_4$	Ti	5.04 mA cm^{-2}	1.41%	This work

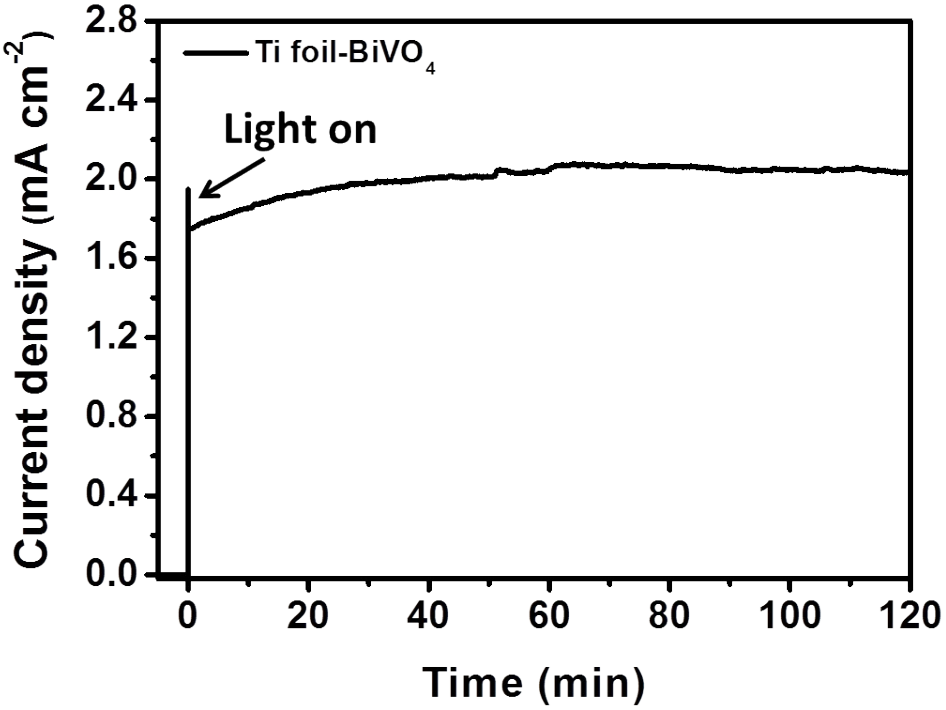

Fig. S12 The Chronoamperometry (*J-t*) curve of Ti foil-$BiVO_4$ collected at 0.6 V_{RHE} in 0.1 M phosphate buffer solution containing 1 M Na_2SO_3 (pH 7.4) under AM 1.5G illumination.

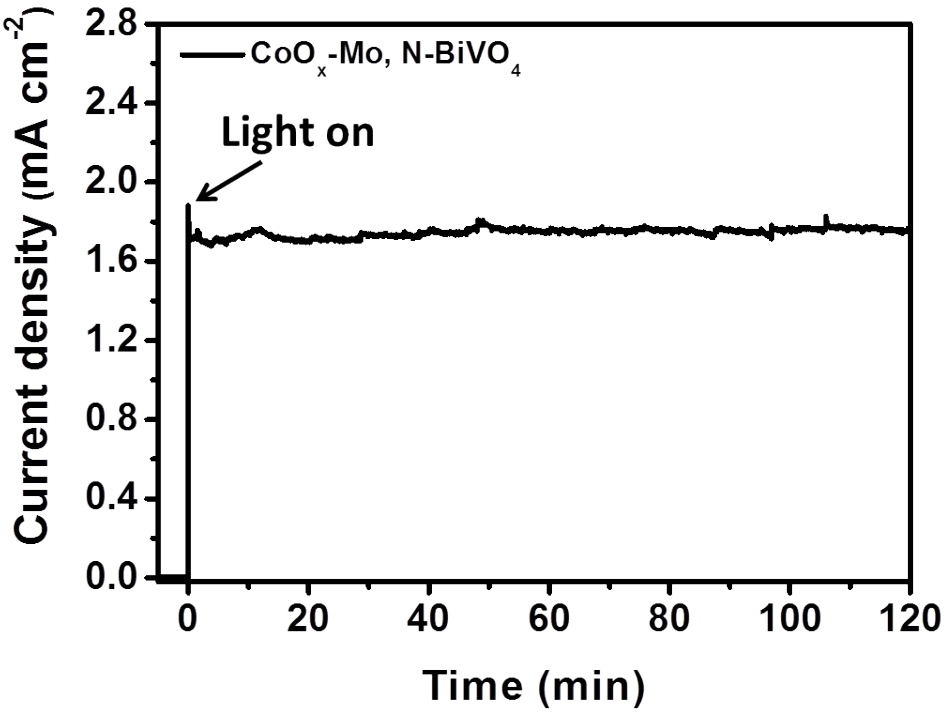

Fig. S13 The Chronoamperometry (*J-t*) curve of CoO_x-Mo, N-$BiVO_4$ collected at 0.6 V_{RHE} in 0.1 M phosphate buffer solution (pH 7.4) without hole scavenger under AM 1.5G illumination.

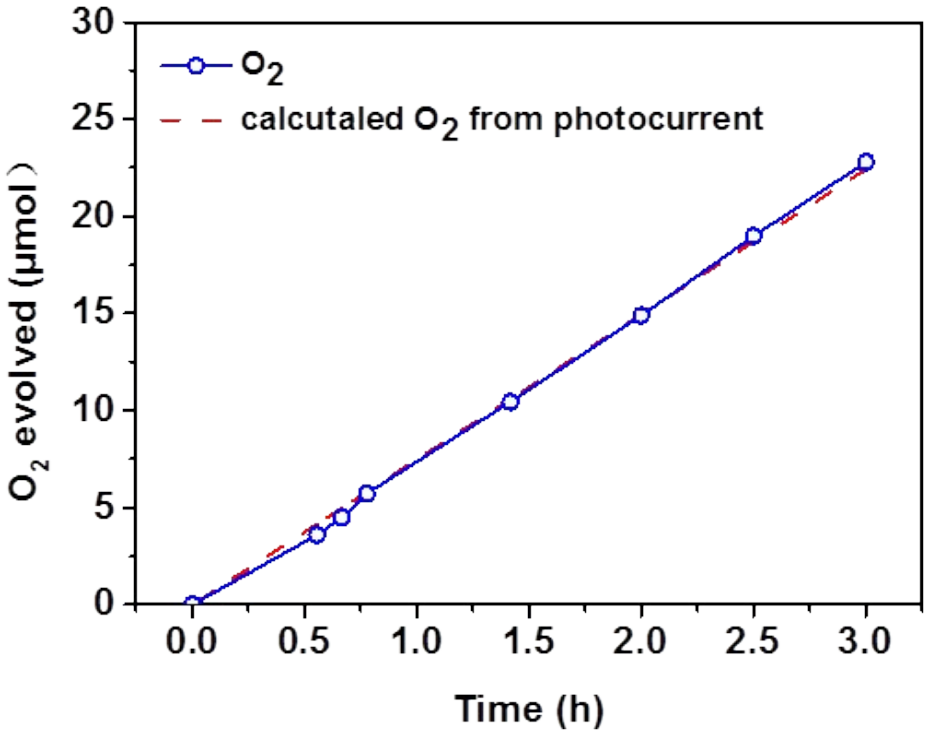

Fig. S14 O_2 produced on the CoO_x-Mo, N-$BiVO_4$ photoanode at 0.6 V_{RHE} in 0.1 M phosphate buffer solution (pH 7.4) under AM 1.5 G illumination.

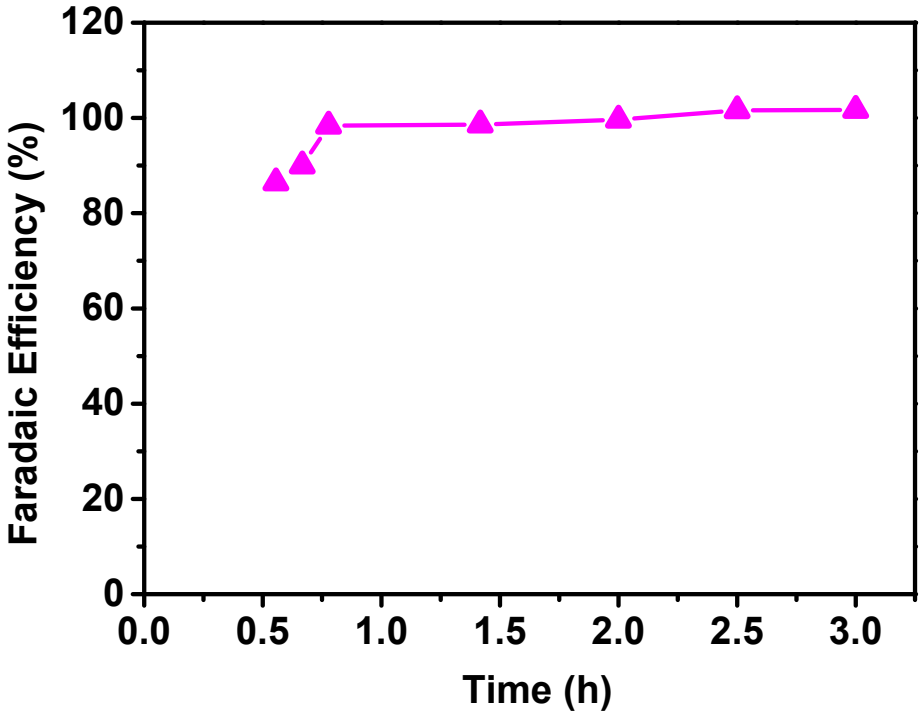

Fig. S15 Faradaic efficiency of CoO_x-Mo, N-$BiVO_4$ photoanode for water oxidation. Solution, 0.1 M phosphate buffer solution (pH 7.4); scan rate, 10 mV s^{-1}; and front illumination (intensity: 100 mW cm^{-2}).

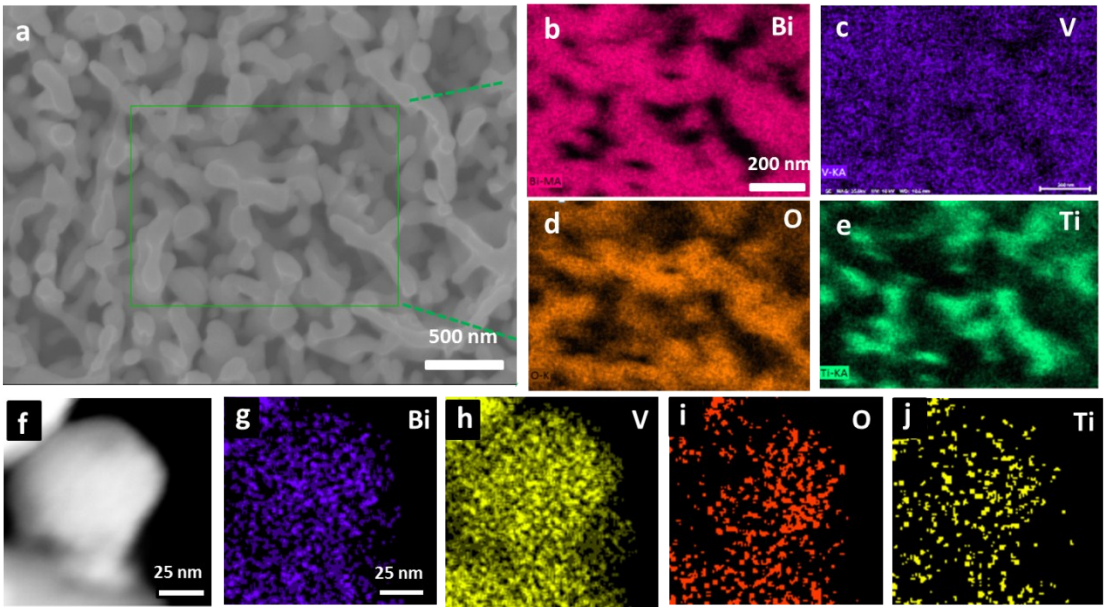

Fig. S16 Electron microscopic characterization of the Ti foil-$BiVO_4$ photoanode.(a) Top-view SEM images of the Ti foil-$BiVO_4$ photoanode and (b-e) SEM-EDS elemental mapping images for Bi, V, O and Ti, respectively; (f) TEM image of Ti foil-$BiVO_4$ and (g-j) TEM-EDS elemental mapping images for Bi, V, O and Ti, respectively.

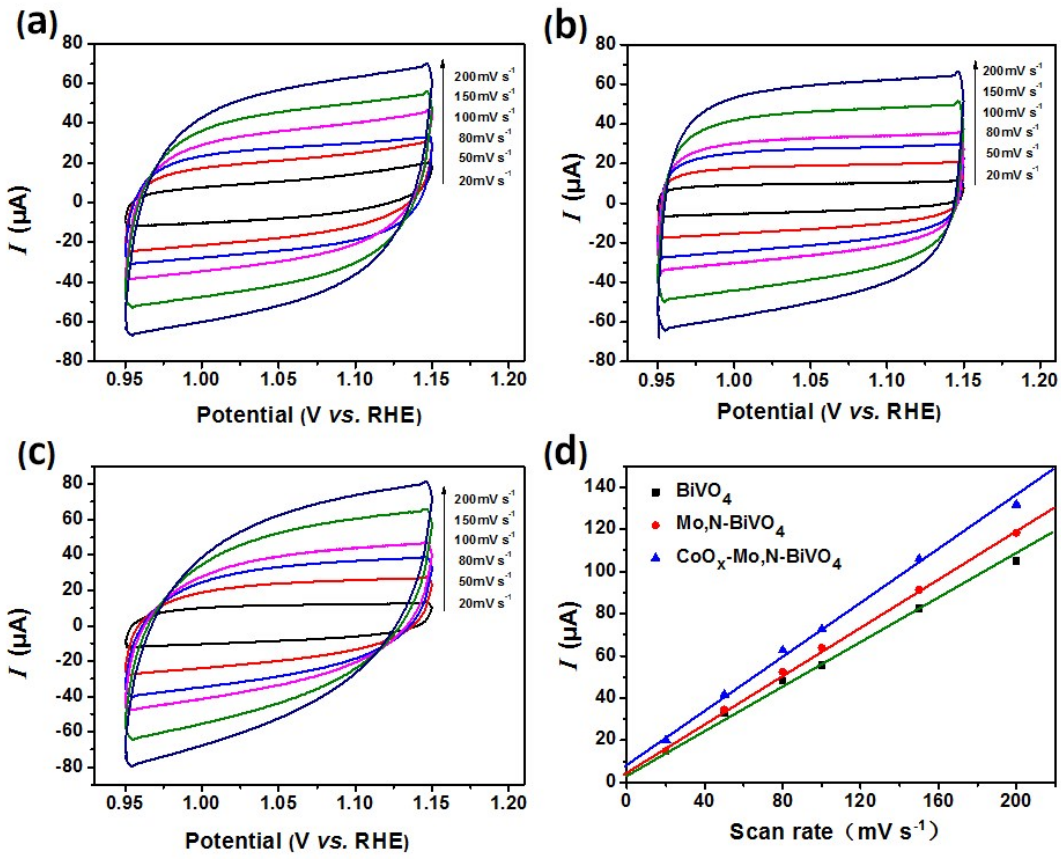

Fig. S17 CV curves measured in a non-Faradaic region of 0.95−1.15 V at various scan rates for (a) $BiVO_4$, (b) Mo, N-$BiVO_4$, (c) CoO_x-Mo, N-$BiVO_4$ with a geometric area of 1 cm^2, respectively. Charging current differences ($\Delta I = I_a - I_c$) measured at 1.05 V plotted against scan rate for $BiVO_4$, Mo,N-$BiVO_4$, and CoO_x-Mo,N-$BiVO_4$, respectively. I_a and I_c are the anodic and cathodic current, respectively, and the linear slope is twice of the double-layer capacitance (C_{dl}).

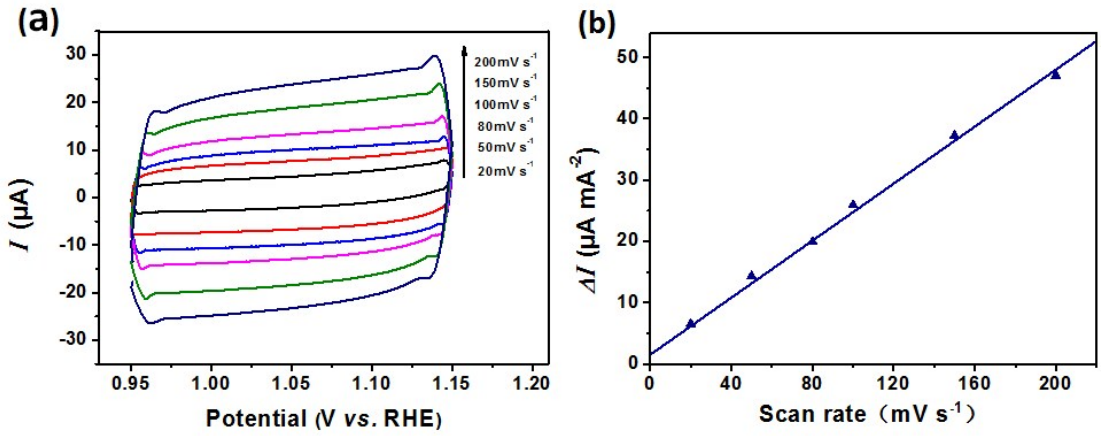

Fig. S18 Double-layer capacitance (C_{dl}) measurements for determining the specific capacitance (C_s) of Ti substrate from cyclic voltammetry (CV) in 0.1 M phosphate buffer solution (a) CV curves measured in a non-Faradaic region of 0.95−1.15 V at various scan rates, (b) Charging current density differences ($\Delta I = I_a - I_c$) measured at 1.05 V plotted against scan rate. I_a and I_c are the anodic and cathodic current density, respectively, and the linear slope is twice of the C_s.

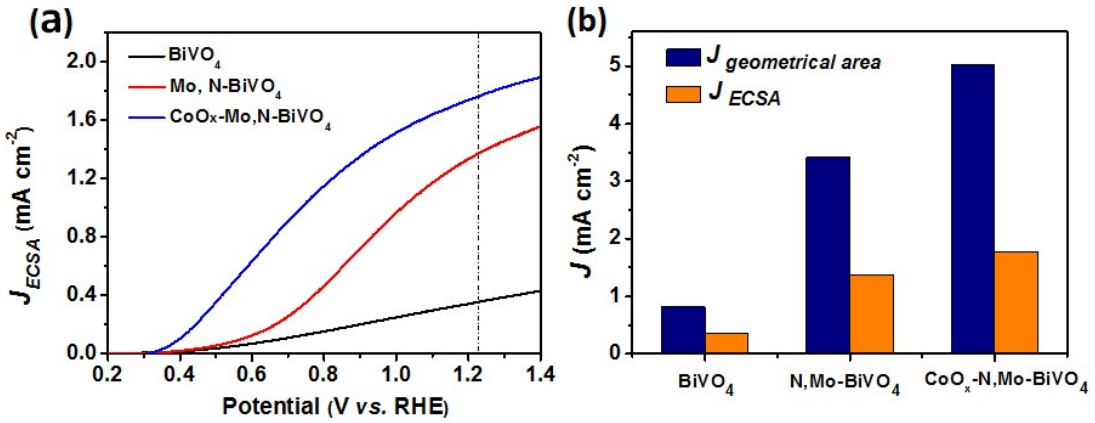

Fig. S19 (a) ECSA normalized photocurrent density vs. voltage curves, and (b) a comparison of the photocurrent density normalized by the geometrical area and the ECSA at 1.23 V_{RHE} for $BiVO_4$, Mo,N-$BiVO_4$, and CoO_x-Mo,N-$BiVO_4$, respectively.